

We are IntechOpen, the world's leading publisher of Open Access books Built by scientists, for scientists

6,900

Open access books available

185,000

International authors and editors

200M

Downloads

Our authors are among the

154

Countries delivered to

TOP 1%

most cited scientists

12.2%

Contributors from top 500 universities



WEB OF SCIENCE™

Selection of our books indexed in the Book Citation Index
in Web of Science™ Core Collection (BKCI)

Interested in publishing with us?
Contact book.department@intechopen.com

Numbers displayed above are based on latest data collected.
For more information visit www.intechopen.com



Evaluation Method for Anisotropic Drilling Characteristics of the Formation by Using Acoustic Wave Information

Deli Gao and Qifeng Pan
*China University of Petroleum at Beijing, Beijing
China*

1. Introduction

In drilling engineering, we must have solid understanding of the underground geological environment which is not only complicated and diversified but also somewhat concealed. Thus, in order to find an effective method of predicting it, a long-term research and practice must be required. In drilling engineering for oil & gas, problems including borehole deviation & its control, wellbore instability & its control, influence directly drilling quality & efficiency of a deep or complicated well for exploration and production of oil & gas fields. For instance, because of the complicated surface and underground conditions as well as the depth (over 5000 m) of oil & gas reservoirs in western China, such unstable factors such as hole deviation and instability often encountered with each other in deep drilling engineering. Because we did not have access to the geological parameters of the formations to be drilled including the rock drillability anisotropy and so on, huge economic loss had been caused and the steps to explore and produce oil & gas in western China had been seriously restricted. Hence, there are many researches and development programs to do for the right cognition and scientific evaluation of the geological environments, and for the further study of mechanism of the drilling process instability, and so on. The solution of these problems is the key to improve the performance of drilling & HSSE (health, safety, security, environment) and lower well construction cost.

The factors influencing the instability can be sorted into subjective category and objective category. In the objective category, there are the types of geological structure and in-situ stress, rock anisotropy, porosity, permeability, lithology, pressures, and mineral components, as well as rock strength and weak layer of the formation to be drilled, and so on. In the subjective category, there are the performance of down hole drilling system, the drilling parameters (weight and torque on bit, etc.), the drilling fluid performances (water loss, viscosity, rheological property and density) and its hydration on shale, the direction and open time of wellbore, the erosion and surge pressure of drilling fluid on the hole wall, the interaction between drillstring and hole wall. Thereby, in researches on the instability, the factors from the both categories should be taken into comprehensive consideration.

Whether in vertical drilling or in directional drilling, it is always a complicated academic and technological problem how to control the well trajectory exactly along the designed

track to reach the underground targets. In rotary drilling, the forming of wellbore & its trajectory is the result of the rock-bit interaction. In this interaction, the drill bit anisotropy and its mechanical behavior (i.e. the drill bit force and tilt angle) are important factors that can directly affect the well trajectory. The mechanical behavior depends on by the bottom hole assembly (BHA) analysis. Accordingly, principal factors influencing the well trajectory generally contain BHA, drill bit, operating parameters in drilling, drilled wellbore configuration and the formations to be drilled. Of which the BHA, drill bit and operating parameters in drilling are the factors that can be artificially controlled, and the formation property (such as rock drillability and its anisotropy) is the objective factor which can not be changed by us. The trajectory can be predicted before drilling and also can be determined after drilling through surveys and calculations. Besides, the drilled wellbore will not only generate a strong reaction on the drill bit force and the drillstring deflection, but also will exert an influence on the anisotropic drilling characteristics of the formation. Due to the above-complicated factors, the hole deviation is always inevitable, which may seriously influence the wellbore quality and the drilling performance.

The well trajectory control is the process which forces drill bit to break through formations along the designed track forward by applying reasonable techniques. The anisotropic drilling characteristics of the drill bit & the formation and their interaction effects are the factors which will cause a direct influence on the well trajectory control. Thereby, it is a complicated scientific and technological problem for us how to make the cognition, evaluation and utilization of anisotropic drilling characteristics of the formation, as well as the prediction & control of mechanical action of the drill bit on the formations.

Rock drillability anisotropy of the formation to be drilled has significant effects on the well trajectory control so that it is very important to evaluate it. Definitions of rock drillability anisotropy and acoustic wave anisotropy of the formation to be drilled are presented in this chapter. The acoustic velocities and the drillability parameters of some rock samples from Chinese Continental Scientific Drilling (CCSD) are respectively measured with the testing device of rock drillability and the ultrasonic testing system in laboratory. Thus, their drillability anisotropy and acoustic wave anisotropy are respectively calculated and discussed in detail by using the experimental data. Based on the experiments and calculations, the correlations between drillability anisotropy and acoustic wave anisotropy of the rock samples are illustrated through regression analysis. What's more, the correlation of rock drillability in directions perpendicular to and parallel to the bedding plane of core samples is studied by means of mathematical statistics. Thus, a mathematic model is established for predicting rock drillability in direction parallel to the formation bedding plane by using rock drillability in direction perpendicular to the formation bedding plane with the well logging or seismic data. The inversion method for rock anisotropy parameters (ϵ, δ) is presented by using well logging information and the acoustic wave velocity in direction perpendicular to the bedding plane of the formation is calculated by using acoustic wave velocity in any direction of the bedding plane. Then, rock drillability in direction perpendicular to the bedding plane of the formation can be calculated by using acoustic wave velocity in the same direction. Thus, rock drillability anisotropy and anisotropic drilling characteristics of the formation can be evaluated by using the acoustic wave information based on well logging data. The evaluation method has been examined by case study based on oilfield data in west China.

2. Anisotropic drilling characteristics of the formation

Although many theories have been proposed to explain the hole deviation since the 1950s (Gao et al, 1994), it is only the rock drillability anisotropy theory (Lubinski & Woods, 1953) that was recognized by petroleum engineers and widely applied to petroleum engineering because it can be used to quantify the anisotropic drilling characteristics of the formation and to explain properly the actual cases of hole deviation encountered in drilling engineering. The theory suggested that since values of rock drillability are not always the same in the directions perpendicular and parallel to the bedding plane of the formation, the formation will bring the bit a considerable force, which may likely cause changes on the original drilling direction and hole deviation.

The orthotropic or the transversely isotropic formations are the typical formations encountered frequently in drilling engineering. The anisotropic effects of the formations (rock drillability) on the well trajectory must be considered in hole deviation control and directional drilling. Based on the rock-bit interaction model, the formation force is defined and modeled in this section to describe quantitatively anisotropic drilling characteristics of the formations to be drilled.

2.1 Definition of rock drillability anisotropy

Because of rock drillability anisotropy, the real drilling direction does not coincide with the resultant force direction of the drill bit (supposed that it is isotropic) on bottom hole. Besides calculating the drill bit force by BHA (bottom hole assembly) analysis, rock drillability anisotropy of the formation must be considered in hole deviation control.

The formation studied here is typical orthotropic one, and the transversely isotropic formation discussed previously is regarded as its particular case. Let \bar{e}_d , \bar{e}_u and \bar{e}_s represent unit vectors in the directions of inner normal, up-dip and strike of the formation respectively, as shown in Fig.1. There are different physical properties along different directions of them. γ in Fig.1 represents dip angle of the formation to be drilled. Rock drillability anisotropy of the formation can be expressed by rock drillability anisotropy index. If the components of penetration rate of the drill bit (isotropic) along inner normal, up-dip and strike of the orthotropic formation are noted as R_{dip} , R_{str} and R_n respectively, correspondingly the net applied forces are F_{dip} , F_{str} and F_n respectively, the rock drillability can be defined as:

$$D_n = \frac{R_n}{F_n}, D_{dip} = \frac{R_{dip}}{F_{dip}}, D_{str} = \frac{R_{str}}{F_{str}} \quad (1)$$

Rock drillability anisotropy of the orthotropic formation may be represented by two indexes (I_{r1} and I_{r2}) which are defined as:

$$I_{r1} = \frac{D_{dip}}{D_n}, I_{r2} = \frac{D_{str}}{D_n} \quad (2)$$

Dip angle and strike of the formation can be obtained from the analysis of well logging and geological structure survey. The values of I_{r1} and I_{r2} for the orthotropic formation can be evaluated by the experimental analysis or using the acoustic wave information.

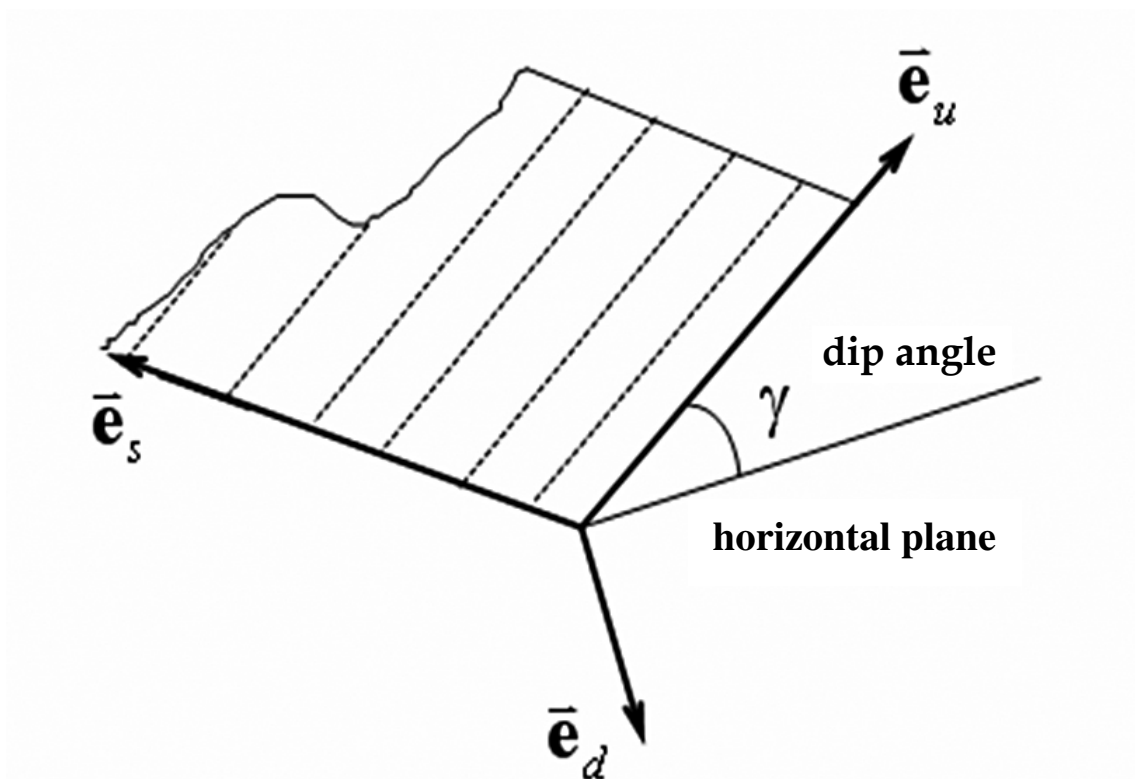


Fig. 1. Descartes coordinates for the formation geometry

2.2 The formation force

Assumed that the drill bit is isotropic for eliminating the effects of its tilt angle on hole deviation, the effects of the orthotropic formation on hole deviation can be presented by the formation force analysis. The two parameter equations related to the formation forces can be derived from the rock-bit interaction model (Gao & Liu, 1989):

$$\begin{cases} G_\alpha = \frac{t_{22}t_{13} - t_{12}t_{23}}{t_{11}t_{22} - t_{12}t_{21}} \\ G_\phi = \frac{t_{11}t_{23} - t_{21}t_{13}}{t_{11}t_{22} - t_{12}t_{21}} \end{cases} \quad (3)$$

Where G_α and G_ϕ are called as the building angle parameter (positive for building up the inclination of well trajectory) and the drifting azimuth parameter (positive for left walking of well trajectory) of the formation respectively, and the t_{ij} ($i, j=1,2,3$) can be expressed as (Gao & Liu, 1990):

$$\begin{cases} t_{ij} = I_{r1}\delta_{ij} + (1 - I_{r1})a_{ij} + (I_{r2} - I_{r1})c_{ij} \\ \delta_{ij} = \begin{cases} 0, & i \neq j \\ 1, & i = j \end{cases} \end{cases} \quad (4)$$

where $a_{ij} = a_{ji}$, $c_{ij} = c_{ji}$ ($i, j=1, 2, 3$) can be calculated by the following equations:

$$\left. \begin{aligned}
 a_{11} &= (\sin \alpha \cos \gamma - \cos \alpha \sin \gamma \cos \Delta \varphi)^2 \\
 a_{12} &= (\cos \alpha \sin \gamma \cos \Delta \varphi - \sin \alpha \cos \gamma) \sin \gamma \sin \Delta \varphi \\
 a_{13} &= (\cos \alpha \sin \gamma \cos \Delta \varphi - \sin \alpha \cos \gamma) (\sin \alpha \sin \gamma \cos \Delta \varphi + \cos \alpha \cos \gamma) \\
 a_{21} &= (\cos \alpha \sin \gamma \cos \Delta \varphi - \sin \alpha \cos \gamma) \sin \gamma \sin \Delta \varphi \\
 a_{12} &= a_{21} \\
 a_{22} &= (\sin \gamma \sin \Delta \varphi)^2 \\
 a_{23} &= \sin \gamma \sin \Delta \varphi (\sin \alpha \sin \gamma \cos \Delta \varphi + \cos \alpha \cos \gamma) \\
 a_{31} &= a_{13} \\
 a_{32} &= a_{23} \\
 a_{33} &= (\sin \alpha \sin \gamma \cos \Delta \varphi + \cos \alpha \cos \gamma)^2
 \end{aligned} \right\} \quad (5)$$

$$\left. \begin{aligned}
 c_{11} &= (\sin \Delta \varphi \cos \alpha)^2 \\
 c_{12} &= -\cos \Delta \varphi \sin \Delta \varphi \cos \alpha \\
 c_{13} &= (\sin \Delta \varphi)^2 \sin \alpha \cos \alpha \\
 c_{21} &= c_{12} \\
 c_{22} &= (\cos \Delta \varphi)^2 \\
 c_{23} &= -\cos \Delta \varphi \sin \Delta \varphi \sin \alpha \\
 c_{31} &= c_{13} \\
 c_{32} &= c_{23} \\
 c_{33} &= (\sin \Delta \varphi \sin \alpha)^2
 \end{aligned} \right\} \quad (6)$$

Where $\Delta \varphi = \varphi - \psi$; φ and α are respectively azimuth and inclination of well trajectory on the bottom hole; γ and ψ are respectively dip angle and up dip azimuth of the formation to be drilled.

It is obviously that the values of G_α and G_ϕ are not only controlled by rock drillability anisotropy of the formation, but also affected by the formation geometry and the well trajectory. Therefore, G_α and G_ϕ can be used to describe the anisotropic drilling characteristics of the formation to be drilled. Thus, the formation force can be mathematically defined as:

$$\begin{cases}
 GF_\alpha = G_\alpha W_{ob} \\
 GF_\phi = G_\phi W_{ob}
 \end{cases} \quad (7)$$

Where GF_α and GF_ϕ are called as the inclination force (positive for building up the inclination) and the azimuth force (positive for decreasing the azimuth) of the formation respectively, and W_{ob} is weight on bit. It should be pointed out that both GF_α and GF_ϕ are only an equivalent expression of anisotropic drilling characteristics of the formation and they are completely different from the mechanical action forces of the drill bit on the formation. Rock drillability anisotropy of the formation is the internal cause of the generations of GF_α and GF_ϕ , while weight on bit is the its external cause.

2.3 G_α and G_ϕ of the transversely isotropic formation

By using equations (5) and (6) and making $I_{r1} = I_{r2} = I_r$, equation (3) can be simplified as the following expressions of G_α and G_ϕ for the transversely isotropic formation:

$$G_\alpha = \frac{(1 - I_r)(\cos \alpha \sin \gamma \cos \Delta \phi - \sin \alpha \cos \gamma)(\cos \alpha \cos \gamma + \sin \alpha \sin \gamma \cos \Delta \phi)}{I_r + (1 - I_r) \left[(\sin \gamma \sin \Delta \phi)^2 + (\cos \alpha \sin \gamma \cos \Delta \phi - \sin \alpha \cos \gamma)^2 \right]} \quad (8)$$

$$G_\phi = \frac{(1 - I_r) \sin \gamma \sin \Delta \phi (\cos \alpha \cos \gamma + \sin \alpha \sin \gamma \cos \Delta \phi)}{I_r + (1 - I_r) \left[(\sin \gamma \sin \Delta \phi)^2 + (\cos \alpha \sin \gamma \cos \Delta \phi - \sin \alpha \cos \gamma)^2 \right]} \quad (9)$$

Where all the symbols here express the same meanings as the previous ones.

3. Experiments on rock anisotropy

Evaluation of rock drillability anisotropy is necessary for hole deviation control in drilling engineering. Many efforts have been made to evaluate rock drillability of the formation through the core testing, the inverse calculation and the acoustic wave. Proposed in this section is an alternative solution by using the acoustic wave to evaluate rock drillability anisotropy of the formation. First, a correlation between the P-wave velocity anisotropy coefficient and the rock drillability anisotropy index of the formation which are calculated according to the core testing data in laboratory, is established by means of mathematical statistics. Then, a mathematical model is obtained for predicting the rock drillability anisotropy index by using the P-wave velocity anisotropy coefficient. Thus, rock drillability anisotropy of the formation can be evaluated conveniently by using the well logging or seismic data (Gao & Pan, 2006).

3.1 Rock drillability anisotropy

3.1.1 Definition

The transversely isotropic formation is a typical anisotropic formation, whose anisotropy can be expressed by a rock drillability anisotropy index:

$$I_r = \frac{D_h}{D_v} \quad (10)$$

where $D_v = V_v/F_v$ and $D_h = V_h/F_h$ are respectively rock drillability parameters in the directions perpendicular and parallel to the bedding plane of the transversely isotropic formation; V_v & F_v and V_h & F_h are the corresponding components of the penetration rate & the net applied force of the isotropic bit to the formation.

When the rock drillability is tested in laboratory using the core samples, the weight on the bit and the rotary speed are constant so that rock drillability anisotropy index of the transversely isotropic formation can also be expressed as:

$$I_r = \frac{T_v}{T_h} \quad (11)$$

where T_v and T_h are two parameters representing the drilling time (seconds) in directions perpendicular and parallel to bedding plane of the core samples respectively. The standard definition of rock drillability can be expressed by the following equation (Yin, 1989):

$$K_d = \log_2 T \quad (12)$$

where K_d is the rock drillability and T the drilling time. Taking two sides of equation (11) into logarithm to the base 2, we can obtain the following equations:

$$\log_2 I_r = \log_2 T_v - \log_2 T_h = K_{dv} - K_{dh} = -\Delta K_d \quad (13)$$

$$I_r = 2^{-\Delta K_d} \quad (14)$$

3.1.2 Rock samples

Fourteen core samples used in laboratory came from the measured depth interval of 48m~1027 m of the well KZ-1 for scientific drilling in China, which were supplied by the Engineering Center for Chinese Continental Scientific Drilling (CCSD). In the directions perpendicular and parallel to the bedding plane, these core samples were cut into shapes of cube or cuboid and their surfaces of both ends were polished and kept parallel to each other, with an error of less than 0.2 mm. Then, the machined samples were put into an oven with a temperature of 105-110°C and roasted for 24 h. Finally, all of the samples can be used for the testing of rock drillability after cooling down to room temperature.

3.1.3 Testing method

The rock drillability can be measured with a device for testing the rock drillability (shown in Fig.2). During the measurement, some weight is applied on the micro-bit by the function of a hydraulic pressure tank with the fixed poises, so that the weight on the micro-bit is kept at a constant value. The measured depth to be drilled to is set with the standard indicator, and the drilling time is logged with a stopwatch. Both the roller bit (bit of this kind has three rotating cones and each cone will rotate on its own axis during drilling) drillability and the PDC (the acronym of Polycrystalline Diamond Compact) bit drillability can be tested with the above-mentioned instrument, which is of the following standard data.

The diameter of the micro-bit is 31.75 mm.

Weight is 90±20 N on the roller bit and 500±20 N on the PDC bit.

The rotary speed is 55±1 r/min.

The total depth to be drilled to is 2.6 mm for the roller bit with a pre-drilled depth of 0.2 mm and 4 mm for the PDC bit with a pre-drilled depth of 1.0 mm.

During testing the rock drillability, the micro-bit is often checked so that each of the worn micro-bits should be replaced in time to ensure the testing accuracy. The testing points of drilling time for each tested side of a rock sample should be gained as many as possible and their average value is taken as the test value of the side. The grade value of each side drillability of the rock sample can be calculated by equation (16) with the test data of drilling time for each side of the rock sample.

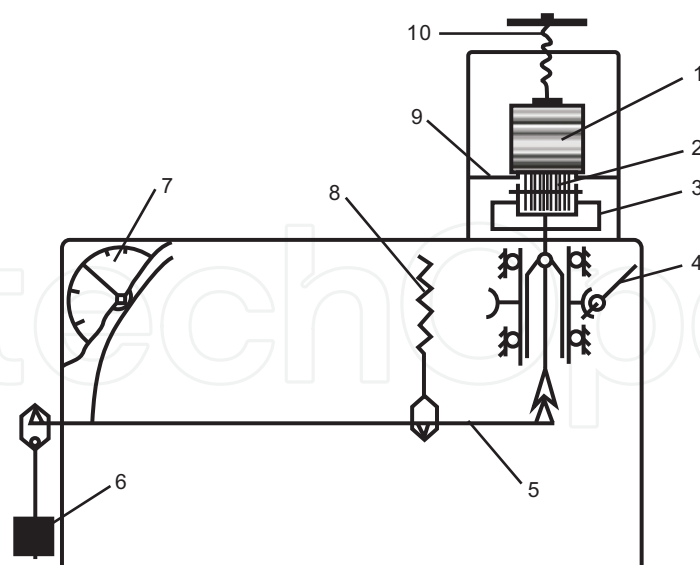


Fig. 2. Testing device for rock drillability (Note: 1. Rock sample; 2. micro-bit; 3. cutting tray; 4. turbine rod; 5. lever; 6. weight; 7. meter for measuring depth; 8. bar with thread for adjusting lever; 9. worktable; 10. compaction bar with thread)

3.1.4 Experimental result and analysis

Some testing results of rock drillability for the 14 core samples from CCSD are obtained in laboratory and shown in Table 1 and Table 2.

No. of the cores from CCSD	Measured depth, m	Rock drillability with the roller bit (K_{dRB})		Rock drillability anisotropy index
		Perpendicular to the bedding plane	Parallel to the bedding plane	
9	48	6.03	6.12	0.94
38	145	9.18	9.86	0.62
57	197	10.29	10.79	0.71
104	305	11.11	11.39	0.82
143	400	8.21	8.17	1.03
179	504	8.70	8.99	0.82
218	607	9.25	10.29	0.49
252	698	10.64	10.78	0.91
281	775	8.78	9.21	0.74
288	795	10.17	8.22	3.86
304	834	7.92	8.57	0.64
340	925	8.89	9.08	0.88
363	998	9.15	10.20	0.48
373	1027	8.12	10.21	0.23

Table 1. Experimental results of rock drillability with the roller bit

No. of the cores from CCSD	Measured depth, m	Rock drillability with the PDC bit (K_{dPDC})		Rock drillability anisotropy index
		Perpendicular to the bedding plane	Parallel to the bedding plane	
9	48	4.55	4.34	1.16
38	145	8.57	10.65	0.24
57	197	9.89	10.06	0.89
104	305	10.78	10.90	0.92
143	400	7.82	7.40	1.34
179	504	8.48	8.47	1.01
218	607	8.61	9.14	0.69
252	698	9.52	9.86	0.79
281	775	8.22	9.03	0.57
288	795	9.55	7.31	4.72
304	834	6.06	7.71	0.32
340	925	8.14	8.95	0.57
363	998	8.18	8.64	0.73
373	1027	7.93	8.77	0.56

Table 2. Experimental results of rock drillability with the PDC bit

It is observed clearly from Table 1 and Table 2 that the rock samples from CCSD have the anisotropic characteristics in the rock drillability. The rock drillability perpendicular to the bedding plan is different from that parallel to the bedding plane, whether it is for the roller bit or for the PDC bit. For the roller bit, indices of drillability anisotropy of the rock samples are ranged from 0.23 to 0.94, except the anisotropy indices of rock samples of 143# and 288#, which are 1.03 and 3.86 respectively. The case is similar to the PDC bit; indices of drillability anisotropy of the rock samples are between 0.24 and 0.92, except the anisotropy indices of rock samples of 9#, 143#, 179# and 288#, corresponding to 1.16, 1.34, 1.01 and 4.72, respectively. Generally, the rock drillability perpendicular to the bedding plan is less than that parallel to the bedding plane, so that the formation can be penetrated more easily in the direction perpendicular to the bedding plane.

3.2 Acoustic anisotropy of rock sample

3.2.1 Definition

It is supposed that the formation is the transversely isotropic, and thus the acoustic anisotropy of the formation rock can be expressed by an acoustic anisotropy index (I_v):

$$I_v = V_{av} / V_{ah} \quad (15)$$

where V_{av} and V_{ah} are the acoustic velocities in rock along the directions perpendicular and parallel to the bedding plane of the formation respectively.

3.2.2 Testing method

With the method of making the ultrasonic pulse penetrating through a rock sample, the acoustic velocities V_{av} and V_{ah} can be measured in laboratory. The ultrasonic testing

system used in laboratory is shown in Fig. 3, in which the ultrasonic transducers can provide a frequency of 0.5 MHz and the butter and honey can be used as its coupling media. The pulse generator can generate electric pulses with a strength range of 1-300 V. The width and iteration frequency of the electric pulse can be adjusted and controlled. During testing, the signal generator makes an electric pulse signal which will touch off the emission end of the energy exchanger to generate ultrasonic pulses. The ultrasonic pulses (acoustic waves) propagating through the rock sample are incepted by the reception end of the energy exchanger. Finally, the propagation time and the signal strength of the ultrasonic pulses (acoustic waves) through the rock sample are logged by a digital memory oscillograph. In order to reduce the errors from the artificial operations, the emission end of the energy exchanger is aimed at its reception end as accurately as possible during testing. Before each test, the ultrasonic testing system should be calibrated using the aluminum rod to ensure the accuracy of the test results. Testing for each point of a rock sample is conducted for three times in the actual testing. The average value of the test data of three times for each point is taken as a final test result for the point of a rock sample. With the test data, the acoustic velocity may be calculated by the following equation:

$$V = \frac{l}{t - t_0} \quad (16)$$

where V is the acoustic velocity; l is length of the rock sample, mm; t is propagation time of the acoustic wave, μs ; and t_0 is delayed time of the testing system, μs .

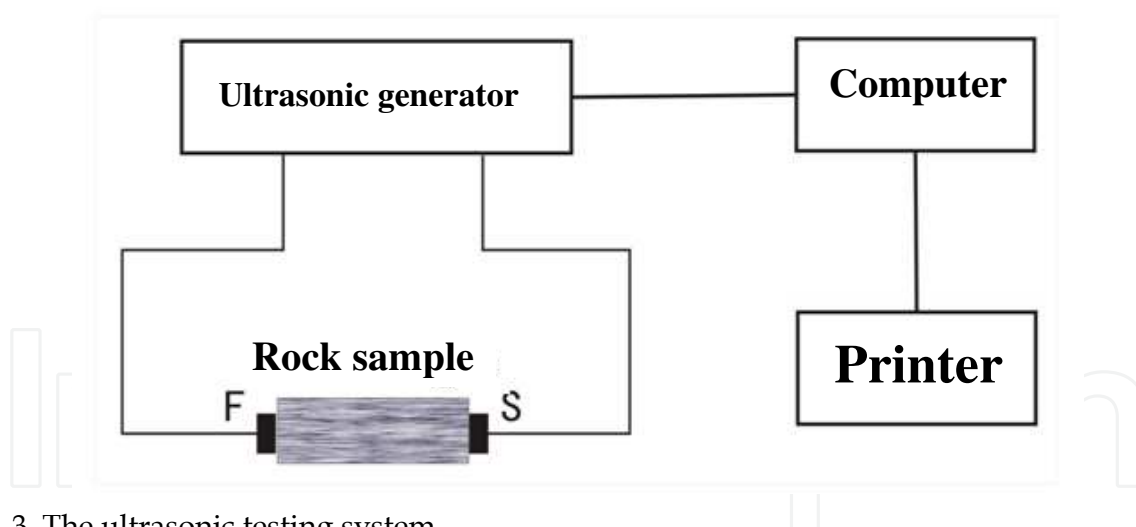


Fig. 3. The ultrasonic testing system

3.2.3 Experimental result and analysis

Some ultrasonic test results of the 14 core samples from CCSD are logged with the above test method and with the ultrasonic testing system in laboratory, and the rock acoustic velocities shown in Table 3 can be calculated by equation (16).

It can be obviously observed from Table 3 that the rock samples from CCSD are of the rock acoustic anisotropy. The rock acoustic velocity perpendicular to the bedding plan is different from that parallel to the bedding plane. Based on the acoustic velocity data in Table 3, the acoustic anisotropy of the rock samples can be calculated by equation (15). The

acoustic anisotropy indices of the rock samples are between 0.85 and 0.98, except the 363# and 373#, which are 0.77 and 0.76 respectively. For the test of the rock samples from CCSD, the rock acoustic velocity perpendicular to the bedding plan is less than that parallel to the bedding plane, as shown in Table 3. The main reason for this difference is that there are many fractures with different scales in the rock sample. When the acoustic wave penetrates through the fractures, the fractures cause a loss of the pulse energy so as to make the acoustic velocity reduce more quickly, on the other hand, the pulse energy is dissipated in the process of propagation. According to some progress in geophysics (Patrick & Richard, 1984), the fractures can play a role in guiding the wave when the elastic wave has propagated in the direction parallel to the bedding plane of the rock sample, and play a role in obstructing the wave when the elastic wave has propagated in the direction perpendicular to the bedding plane. Therefore, the propagation of the acoustic wave penetrating through the rock sample is probably controlled by such a kind of geophysical mechanism.

No. of the core from CCSD	Measured depth, m	P-wave velocities of the rock samples, m/s		Acoustic anisotropy index of the rock sample
		Perpendicular to bedding plane (V_{av})	Parallel to bedding plane (V_{ah})	
9	48	4387	4457	0.98
38	145	4442	5120	0.87
57	197	6365	6826	0.93
104	305	5431	5714	0.95
143	400	4410	4928	0.89
179	504	4568	4744	0.96
218	607	4177	4671	0.89
252	698	5805	5990	0.97
281	775	4776	5516	0.87
288	795	5142	5453	0.94
304	834	4392	5129	0.86
340	925	4325	5096	0.85
363	998	3816	4928	0.77
373	1027	3761	4930	0.76

Table 3. Experimental results of acoustic velocities of the rock samples

3.3 Correlations between I_r and I_v

With the experimental data in table 1 to table 3 and the corresponding calculations, it can be found that the rock drillability anisotropy is inherently related to the acoustic anisotropy of the rock samples. Therefore, exponential function, logarithmic function, polynomial function, and linear function, are used to make a regression analysis of the data obtained by experiments. With the matching & extrapolating effects of these regression functions comprehensively considered, exponential function is finally selected as the regression model of correlation between I_r and I_v . The results of regression calculations for the correlations are listed in Table 4.

In Table 4, I_{rRB} is denoted as the drillability anisotropy index of the rock sample with a roller bit, I_{vp} as the acoustic anisotropy index of P-wave through the rock sample, ΔK_{dRB} as

the rock drillability difference between both directions perpendicular and parallel to the bedding plane of the rock sample with a roller bit, calculated by equation (13), and I_{rPDC} as the drillability anisotropy index of the rock sample with a PDC bit.

Regression functions		$I_{rRB} = e^{(a+bl_{vp})}$	$\Delta K_{dRB} = e^{(a+bl_{vp})}$	$I_{rPDC} = e^{(a+bl_{vp})}$
a	Value	-3.418	8.129	-4.286
	Standard error	0.840	1.893	1.491
	t-ratio	-4.0679	4.295	-2.875
	Prob.(t)	0.00226	0.00157	0.02068
b	Value	3.401	-9.993	4.366
	Standard error	0.914	2.361	1.661
	t-ratio	3.721	-4.232	2.628
	Prob.(t)	0.00397	0.00174	0.03026
Correlation coefficient R		0.793	0.832	0.710
F-ratio		16.92	22.41	8.09
Prob.(F)		0.0021	0.0008	0.0217

Table 4. Results of the regression calculations

4. Evaluation method based on acoustic wave information

Many studies have been made to evaluate the rock drillability anisotropy with the core testing method (Gao & Pan, 2006) and the inversion method (Gao et al, 1994). However, as for the core testing method, its result may not reflect the actual rock drillability anisotropy since the experimental conditions are different from the downhole conditions. Moreover, the profile of rock drillability anisotropy along the hole depth can not be established because of the limitation of the core samples. The inversion method needs to work with a bottom hole assembly (BHA) analysis program and some parameters in the inversion model are not easy to obtain so that its applications are limited to some extent. Thus, the evaluation method will be presented in this section so as to predict rock drillability anisotropy of the formation by using the acoustic wave information (Gao et al, 2008).

4.1 Acoustic wave velocity of the formation

The formation studied here is the transversely isotropic formation which is frequently encountered in drilling for oil & gas. Experimental investigation shows that layered rock has the transversely isotropic characteristics.

4.1.1 Phase velocity in the transversely isotropic formation

For the transversely isotropic media, Hooke's law can be written as

$$\begin{pmatrix} \sigma_{xx} \\ \sigma_{yy} \\ \sigma_{zz} \\ \sigma_{yz} \\ \sigma_{xz} \\ \sigma_{xy} \end{pmatrix} = \begin{pmatrix} C_{11} & C_{11} - 2C_{66} & C_{13} & 0 & 0 & 0 \\ C_{11} - 2C_{66} & C_{11} & C_{13} & 0 & 0 & 0 \\ C_{13} & C_{13} & C_{33} & 0 & 0 & 0 \\ 0 & 0 & 0 & C_{44} & 0 & 0 \\ 0 & 0 & 0 & 0 & C_{44} & 0 \\ 0 & 0 & 0 & 0 & 0 & C_{66} \end{pmatrix} \begin{pmatrix} \epsilon_{xx} \\ \epsilon_{yy} \\ \epsilon_{zz} \\ \epsilon_{yz} \\ \epsilon_{xz} \\ \epsilon_{xy} \end{pmatrix} \quad (17)$$

Elastodynamic equation of the elastic media can be obtained from the textbook and expressed as

$$\begin{cases} \frac{\partial \sigma_{xx}}{\partial x} + \frac{\partial \sigma_{yx}}{\partial y} + \frac{\partial \sigma_{zx}}{\partial z} + X - \rho \frac{\partial^2 u}{\partial t^2} = 0 \\ \frac{\partial \sigma_{yy}}{\partial y} + \frac{\partial \sigma_{zy}}{\partial z} + \frac{\partial \sigma_{xy}}{\partial x} + Y - \rho \frac{\partial^2 v}{\partial t^2} = 0 \\ \frac{\partial \sigma_{zz}}{\partial z} + \frac{\partial \sigma_{xz}}{\partial x} + \frac{\partial \sigma_{yz}}{\partial y} + Z - \rho \frac{\partial^2 w}{\partial t^2} = 0 \end{cases} \quad (18)$$

where X , Y , and Z are respectively the body force in directions of x , y and z (Xu, 2011). u , v and w are the corresponding displacements. ρ is the density of the elastic media, g / cm^3 . Substituting equation (17) into equation (18) and solving with geometric equations without considering body force, we can get the following wave equation :

$$\begin{cases} \rho \frac{\partial^2 u}{\partial t^2} = C_{11} \frac{\partial^2 u}{\partial x^2} + C_{66} \frac{\partial^2 u}{\partial y^2} + C_{44} \frac{\partial^2 u}{\partial z^2} + (C_{11} - C_{66}) \frac{\partial^2 v}{\partial x \partial y} + (C_{13} + C_{44}) \frac{\partial^2 w}{\partial x \partial z} \\ \rho \frac{\partial^2 v}{\partial t^2} = C_{66} \frac{\partial^2 v}{\partial x^2} + C_{22} \frac{\partial^2 v}{\partial y^2} + C_{44} \frac{\partial^2 v}{\partial z^2} + (C_{11} - C_{66}) \frac{\partial^2 u}{\partial x \partial y} + (C_{13} + C_{44}) \frac{\partial^2 w}{\partial y \partial z} \\ \rho \frac{\partial^2 w}{\partial t^2} = C_{44} \frac{\partial^2 w}{\partial x^2} + C_{44} \frac{\partial^2 w}{\partial y^2} + C_{33} \frac{\partial^2 w}{\partial z^2} + (C_{13} + C_{44}) \frac{\partial^2 u}{\partial x \partial z} + (C_{13} + C_{44}) \frac{\partial^2 v}{\partial y \partial z} \end{cases} \quad (19)$$

Because of the symmetry of the stress and strain in the direction normal to z direction, the wave equation can be simplified to two dimensions without any loss of generality. In the plane of $y=0$ (that is the xz plane), the wave equation (19) can be written as

$$\begin{cases} \rho \frac{\partial^2 u}{\partial t^2} = C_{11} \frac{\partial^2 u}{\partial x^2} + C_{44} \frac{\partial^2 u}{\partial z^2} + (C_{13} + C_{44}) \frac{\partial^2 w}{\partial x \partial z} \\ \rho \frac{\partial^2 v}{\partial t^2} = C_{66} \frac{\partial^2 v}{\partial x^2} + C_{44} \frac{\partial^2 v}{\partial z^2} \\ \rho \frac{\partial^2 w}{\partial t^2} = C_{44} \frac{\partial^2 w}{\partial x^2} + C_{33} \frac{\partial^2 w}{\partial z^2} + (C_{13} + C_{44}) \frac{\partial^2 u}{\partial x \partial z} \end{cases} \quad (20)$$

The solutions of equation (20) are

$$\rho v_{Pa}^2(\theta) = \frac{1}{2}[C_{33} + C_{44} + (C_{11} - C_{33})\sin^2 \theta + D(\theta)] \quad (21)$$

$$\rho v_{SVa}^2(\theta) = \frac{1}{2}[C_{33} + C_{44} + (C_{11} - C_{33})\sin^2 \theta - D(\theta)] \quad (22)$$

$$\rho v_{SHa}^2(\theta) = C_{66} \sin^2 \theta + C_{44} \cos^2 \theta \quad (23)$$

Where

$$D(\theta) = \{(C_{33} - C_{44})^2 + 2[2(C_{13} + C_{44})^2 - (C_{33} - C_{44})(C_{11} + C_{33} - 2C_{44})]\sin^2 \theta + [(C_{11} + C_{33} - 2C_{44})^2 - 4(C_{13} + C_{44})^2]\sin^4 \theta\}^{1/2}$$

where v_{Pa} is phase velocity of the P-wave; v_{SVa} is phase velocity of P-SV wave; v_{SHa} is phase velocity of SH-wave; θ is phase angle which is the angle between the wave front normal and the unique (vertical) axis as shown in Fig.4.

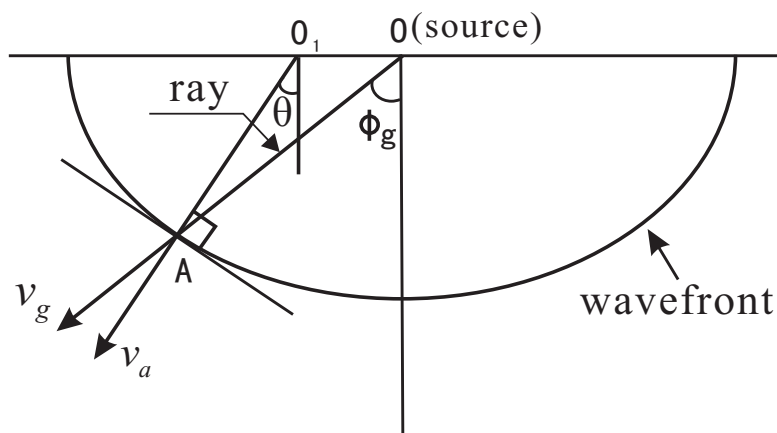


Fig. 4. Phase angle and group angle

It is defined that

$$\varepsilon = \frac{C_{11} - C_{33}}{2C_{33}} \quad (24)$$

$$\gamma = \frac{C_{66} - C_{44}}{2C_{44}} \quad (25)$$

$$\delta^* = \frac{1}{2C_{33}^2} [2(C_{13} + C_{44})^2 - (C_{33} - C_{44})(C_{11} + C_{33} - 2C_{44})] \quad (26)$$

and

$$\alpha_0 = \sqrt{C_{33} / \rho} \quad , \quad \beta_0 = \sqrt{C_{44} / \rho} \quad (27)$$

where α_0 is the vertical P-wave velocity; β_0 is the vertical SV-wave velocity; ρ is rock density. ε , γ and δ^* are rock anisotropy parameters of the formation. Substituting equation (24), (25), (26) and (27) into equation (21), (22) and (23), we can get

$$v_{Pa}^2(\theta) = \alpha_0^2[1 + \varepsilon \sin^2 \theta + D^*(\theta)], \quad (28)$$

$$v_{SVa}^2(\theta) = \beta_0^2[1 + \frac{\alpha_0^2}{\beta_0^2} \varepsilon \sin^2 \theta - \frac{\alpha_0^2}{\beta_0^2} D^*(\theta)] \quad (29)$$

$$v_{SHa}^2(\theta) = \beta_0^2[1 + 2\gamma \sin^2 \theta] \quad (30)$$

where

$$D^*(\theta) = \frac{1}{2} \left(1 - \frac{\beta_0^2}{\alpha_0^2}\right) \left\{ \left[1 + \frac{4\delta^*}{(1 - \beta_0^2 / \alpha_0^2)^2} \sin^2 \theta \cos^2 \theta + \frac{4(1 - \beta_0^2 / \alpha_0^2 + \varepsilon)\varepsilon}{(1 - \beta_0^2 / \alpha_0^2)^2} \sin^4 \theta\right]^{1/2} - 1 \right\} \quad (31)$$

Letting $\theta = \frac{\pi}{2}$ and substituting it into equations (28), (29), (30) and (31), we can get

$$\begin{cases} v_{Pa,90} = \alpha_0 (1 + 2\varepsilon)^{0.5} \\ v_{SVa,90} = \beta_0 \\ v_{SHa,90} = \beta_0 (1 + 2\gamma)^{0.5} \end{cases} \quad (32)$$

For the case of weak rock anisotropy (i.e. the quantity of ε , γ , θ and δ^* is small), expanding equation (31) in the Taylor series at fixed θ and neglecting the second order of small quantity can be simplified as

$$D^* \approx \frac{\delta^*}{(1 - \beta_0^2 / \alpha_0^2)} \sin^2 \theta \cos^2 \theta + \varepsilon \sin^4 \theta \quad (33)$$

Using equations (33) in equation (28) and (29), expanding v_{Pa} , v_{SVa} and v_{SHa} in a Taylor series at the fixed θ and neglecting the second order of small quantity can be expressed as

$$v_{Pa}(\theta) = \alpha_0(1 + \delta \sin^2 \theta \cos^2 \theta + \varepsilon \sin^4 \theta) \quad (34)$$

$$v_{SVa}(\theta) = \beta_0[1 + \frac{\alpha_0^2}{\beta_0^2}(\varepsilon - \delta) \sin^2 \theta \cos^2 \theta] \quad (35)$$

$$v_{SHa}(\theta) = \beta_0(1 + \gamma \sin^2 \theta) \quad (36)$$

Where

$$\delta = \frac{1}{2} \left[\varepsilon + \frac{\delta^*}{(1 - \beta_0^2 / \alpha_0^2)} \right].$$

4.1.2 Phase velocity and group velocity

The phase velocity is the velocity in the direction of the phase propagation vector, normal to the surface of constant phase, which is also called the wave front velocity since it is the propagation velocity of the wave front along the phase vector. The phase angle is formed between the direction of phase vector and the vertical axis. In contrast, the ray vector points always from the source to the considered point on the wave front. The energy propagates along the ray vector with the group velocity, while the group angle is formed between the propagation direction and the vertical axis. The difference between the phase angle and the ray angle is illustrated in Fig.4.

The relationship between the phase angle and the group angle can be expressed by the following equation:

$$\tan(\phi_g - \theta) = \frac{dv_a}{v_a d\theta} \quad (37)$$

Where ϕ_g is the group angle; v_a is the phase velocity; θ is the phase angle. Expanding equation (37) leads to

$$\tan(\phi_g(\theta)) = (\tan \theta + \frac{1}{v_a} \frac{dv_a}{d\theta}) / (1 - \frac{\tan \theta}{v_a} \frac{dv_a}{d\theta}) \quad (38)$$

The group velocity (v_g) is related to the phase velocity (v_a) as shown by the following formula

$$v_g^2(\phi_g(\theta)) = v_a^2(\theta) + \left(\frac{dv_a}{d\theta}\right)^2 \quad (39)$$

Where v_g is the group velocity.

The following section makes the solution for the relationship between the group velocity and the phase velocity, the group angle and the phase angle of the P-wave at any angle.

Another rock anisotropy parameter δ is introduced and expressed as

$$\delta = \frac{1}{2} \left[\varepsilon + \frac{\delta^*}{(1 - \beta_0^2 / \alpha_0^2)} \right] = \frac{(C_{13} + C_{44})^2 - (C_{33} - C_{44})^2}{2C_{33}(C_{33} - C_{44})} \quad (40)$$

Letting $t = 1 - \beta_0^2 / \alpha_0^2$, equation (38) can be rescaled as

$$\frac{v_{Pa}^2(\theta)}{\alpha_0^2} = 1 + \varepsilon \sin^2 \theta + D(\theta) \quad (41)$$

Where

$$D(\theta) = \frac{1}{2} \sqrt{4(\varepsilon^2 + 2t\varepsilon - 2t\delta) \sin^4 \theta + 4t(2\delta - \varepsilon) \sin^2 \theta + t^2} - \frac{1}{2} t .$$

Making derivation to both sides of equation (41), we can get

$$\frac{dv_{pa}(\theta)}{d\theta} = \frac{\alpha_0^2 \sin \theta \cos \theta}{v_{pa}(\theta)R(\theta)} \left[2(\varepsilon^2 + 2\varepsilon t - 2t\delta) \sin^2 \theta + 2t\delta - \varepsilon t + \varepsilon R(\theta) \right] \quad (42)$$

Where

$$R(\theta) = \left(4(\varepsilon^2 + 2\varepsilon t - 2t\delta) \sin^4 \theta + 4t(2\delta - \varepsilon) \sin^2 \theta + t^2 \right)^{\frac{1}{2}} = 2D(\theta) + t.$$

Substituting equations (41) and (42) into equation (38), we can get

$$\tan \phi_g = \frac{\{2[M_3(\theta) - M_2(\theta) - 2M_1] \sin^2 \theta - M_4(\theta) - 2M_3(\theta)\} \tan \theta}{2[M_3(\theta) - M_2(\theta)] \sin^2 \theta - M_4(\theta)} \quad (43)$$

Where

$$M_1 = \varepsilon^2 - 2t\delta + 2t\varepsilon;$$

$$M_2(\theta) = 4t\delta + \varepsilon R(\theta) - 2t\varepsilon;$$

$$M_3(\theta) = 2t\delta + \varepsilon R(\theta) - t\varepsilon;$$

$$M_4(\theta) = t^2 - tR(\theta) + 2R(\theta).$$

Substituting equation (41) and (42) into equation (39), we can get the following equation:

$$v_{pg}(\phi_g(\theta)) = \frac{1}{v_{pa}(\theta)R(\theta)} \left\{ v_{pa}^4(\theta)R^2(\theta) + \alpha_0^4 \sin^2 \theta \cos^2 \theta \left[2M_1 \sin^2 \theta + M_3(\theta) \right]^2 \right\}^{\frac{1}{2}} \quad (44)$$

Where v_{pg} is the group velocity of the P-wave; v_{pa} is the phase velocity of the P-wave.

In the case of $\theta = 0^\circ$ and $\theta = 90^\circ$, $\frac{dv_{pa}(\theta)}{d\theta} = 0$, the phase velocity is equal to the group velocity. Thus, when the group angle of the P-wave at the considered point of the formation is given, its phase angle can be calculated by using equation (43). Phase velocity and group velocity of the point can also be made out by using equation (41) and (44).

4.1.3 Methodology for determining rock anisotropy parameters

From the above discussion, we know that if rock anisotropy parameters δ , ε and γ , are known, the wave velocity at any direction can be calculated by using acoustic wave velocity perpendicular to the bedding of the formation. In other words, the acoustic wave velocity perpendicular to the bedding of the formation can be made out if the wave velocity at any direction and rock anisotropy parameters, δ , ε and γ , are known.

It is assumed that the formation to be drilled is transversely isotropic with symmetry axis perpendicular to the bedding of the formation and the formation properties do not change significantly from one well to another. Acoustic wave logging provides a way to measure the velocity of P-wave or S-wave in the formation (or slowness time). The schematic figure for measuring the velocity of P-wave or S-wave is illustrated in Fig.5.

In the figure 5, S_1 and S_2 are monopole sonic transducers. R_1 , R_2 , R_3 and R_4 are sonic receivers. When the sonic is transmitted from S_1 , time difference between R_2 and R_4 is recorded. In the same way, when the sonic is transmitted from S_2 , time difference between R_1 and R_3 is recorded. The average of time difference between R_2 and R_4 and time difference between R_1 and R_3 is the velocity in the formation measured.

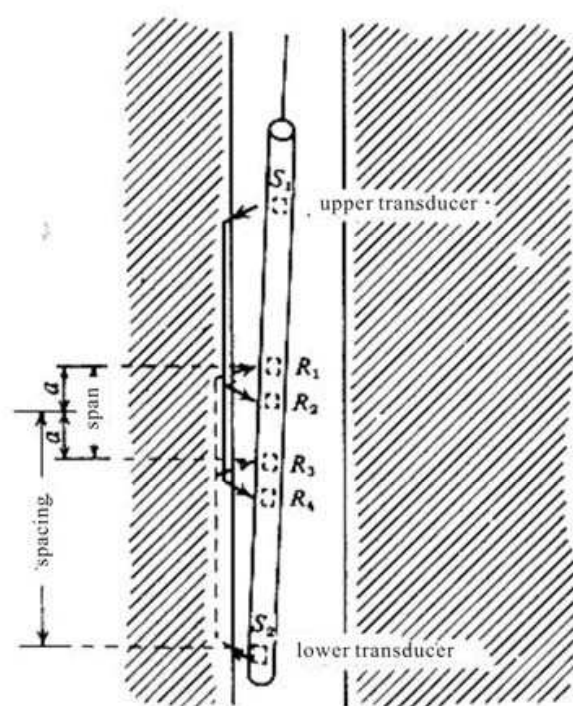


Fig. 5. The principle of acoustic wave logging

Since available S-wave velocity is limited in logging data, we restrict ourselves to take consideration of the P-wave only. The frequency of the acoustic wave logging is about 20kHz~25kHz, which has long wave length. Since a monopole sonic transducer has a mini-bulk, a monopole borehole sonic tool may be approximated by a point source in line with an array of point receivers. The group velocity surface is the response from a point source and so the monopole sonic tool response is approximated as a point source coupled with a series of point receivers in an infinite media (neglecting borehole effects). Therefore, we measure group velocity with borehole sonic tools.

Three parameters, the vertical P-wave velocity (α_0) and the anisotropy parameters ε and δ can be recovered using borehole sonic measurement at different angles relative to the axis of symmetry by following objective function:

$$\Delta v_p = \frac{1}{n} \sum_{i=1}^n [v_{p_{mi}}(\theta) - v_{p_{ci}}(\theta)]^2 \quad (45)$$

where $v_{p_{mi}}(\theta)$ is the measured P-wave velocity; $v_{p_{ci}}(\theta)$ is the P-wave velocity calculated by equation (32); n is the total number of the measured signals. The goal of the inversion is to find the optimization value of C_{11} , C_{13} , C_{33} and C_{44} , to minimize value of Δv_p , by which α_0 , δ and ε can be calculated, as shown in Fig.6 (Gao et al, 2008).

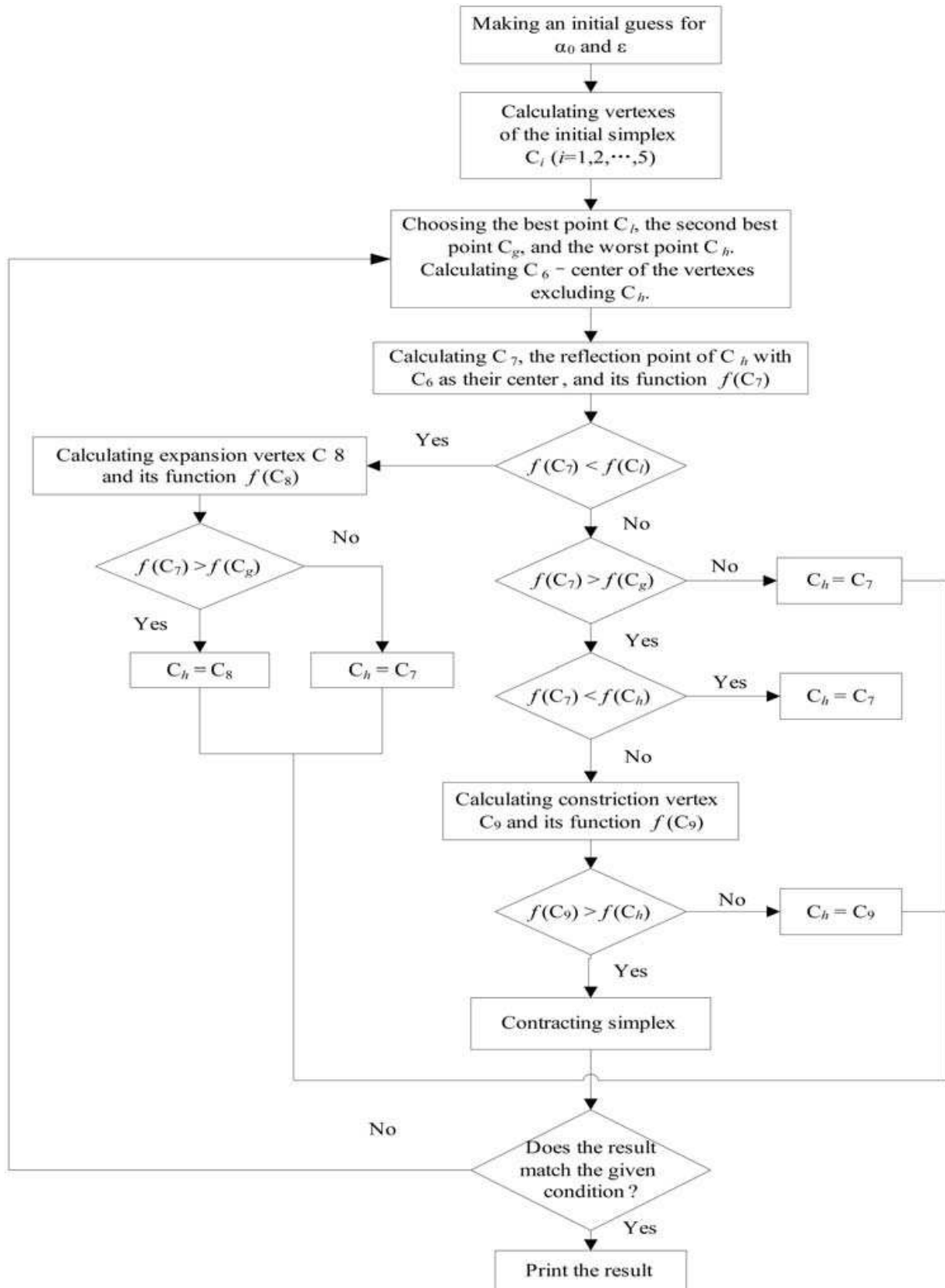


Fig. 6. Flow chart for the inversion calculations of rock anisotropy parameters

4.2 Prediction model of rock drillability anisotropy

Based on the previous section 3, a calculation model has been established to predict rock drillability anisotropy of the formation:

$$I_r = 2^{C_1 K_{dv} + C_2} \quad (46)$$

$$K_{dv} = C_3 + C_4 \ln(\Delta t) \quad (47)$$

Where K_{dv} is the rock drillability perpendicular to the bedding plane of the formation; Δt is the time interval of acoustic wave in the same direction, us/m; C_j ($j=1,2,3,4$) are the regression coefficients based on the experimental data and the survey data in drilling engineering. For example, by the regression analysis based on some oilfield data in west China, we can get such coefficients as $C_1=0.05246$, $C_2=-0.76732$, $C_3=32.977$, $C_4=-4.950$.

4.3 Evaluation method of rock drillability anisotropy based on acoustic wave

From equations (46) and (47), it is shown that the key point for the evaluation of rock drillability anisotropy is how to obtain the rock drillability perpendicular to the bedding plane of the formation which depends on the time interval of acoustic wave in the same direction. Thus, the evaluation of rock drillability anisotropy comes down to determine the time interval of acoustic wave perpendicular to the bedding plane of the formation.

Provided that the formation is of the transversely isotropy and has the symmetry axis perpendicular to the bedding plane of the formation, the angle between hole axis and the formation normal can be calculated by the following formula which is derived from transformation of the formation coordinates to the bottom hole coordinate.

$$\omega = \arccos[\cos \alpha \cos \beta - \sin \alpha \sin \beta \cos(\phi - \phi_f)] \quad (48)$$

where ω is the angle between hole axis and normal of the formation; α is hole inclination, degree or radian; ϕ is azimuth, degree or radian; β is stratigraphic dip, degree or radian; ϕ_f is azimuth of the formation tendency, degree or radian.

When rock anisotropy parameters of a hole section is known, its acoustic wave velocity perpendicular to the bedding plane of the formation can be calculated by the following procedures:

1. Calculating group angle according to stratigraphic dip angle & up dip direction, and inclination & azimuth of hole.
2. Making an initial guess for the acoustic wave velocity $v_{p,0}$.
3. Reading shear wave velocity from shear wave logging or calculating it by equation (46).
4. Calculating phase angle by equation (43).
5. Calculating phase velocity and group velocity of the P-wave by equation (41) and equation (44), respectively.
6. Comparing the P-wave group velocity with the measured velocity.
7. If group velocity of the P-wave matches the measured velocity, $v_{p,0}$ is what we find. Otherwise, we should repeat step 2 to step 7 until they are matched.

The flow chart for inversion of the acoustic wave velocity perpendicular to the bedding plane of the formation is shown in figure 7.

The rock drillability can be calculated by equation (47) after obtaining the time interval of the acoustic wave perpendicular to the bedding plane of the formation. Thus, the profile of rock drillability anisotropy index can be established by using equation (46).

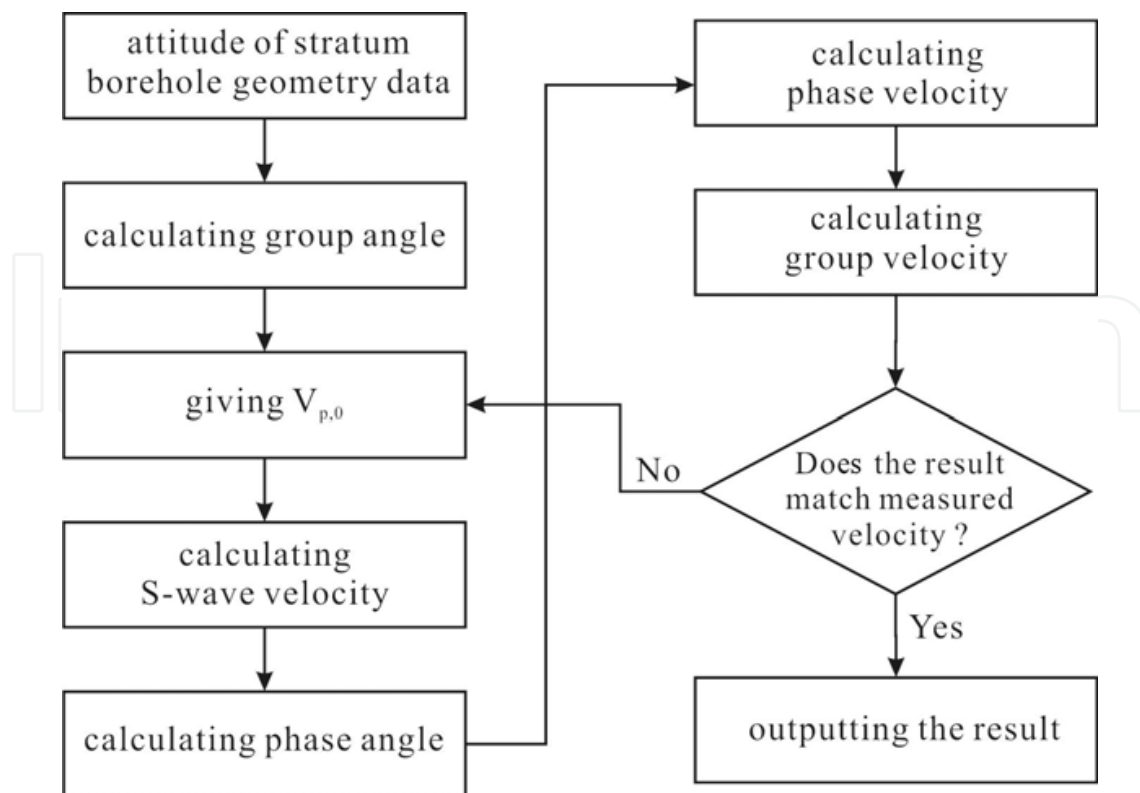


Fig. 7. Inversion method of the acoustic wave velocity perpendicular to the bedding plane

5. Case study

Based on some well logging data and drilling information from Qinghai oilfield in west China, the case study is presented in this section to verify the evaluation method for the anisotropic drilling characteristics of the formation to a certain extent.

Based on these data in table 5, rock drillability anisotropy of the formation and its anisotropic drilling characteristics can be calculated by using the evaluation method described above. The inversion result of shale anisotropy parameters is shown in table 6.

Well Number	Well logging information
Well 5	gamma-ray, compensated acoustic wave and compensated density, inclinometer data and geologic stratification data
Well 6	gamma-ray, compensated acoustic wave and compensated density, inclinometer data and geologic stratification data
Well 7	gamma-ray, compensated acoustic wave and compensated density, inclinometer data and geologic stratification data, and some other records

Table 5. Well drilling & logging information from some completed wells at the Honggouzi conformation in Qinghai oilfield

$v_{P,0}$ (m/s)	ε	δ	root-mean-square (m/s)
4029.1	1.6833	1.6098	98.6153

Table 6. The inversion result of shale anisotropy parameters for the Honggouzi conformation

From the data in the table 6, we can see that the shale is of strong rock anisotropy. The acoustic wave front of the shale section is shown in figure 8.



Fig. 8. Acoustic wave front of the shale section of the Honggouzi conformation

Based on the wave front of the shale shown in Fig.8, the rock anisotropy parameters of the formation at any measured depth, ε and δ , can be approximately calculated by the following equations:

$$\left. \begin{aligned}
 \varepsilon &= V_{sh} \varepsilon_c \\
 \delta &= V_{sh} \delta_c \\
 V_{sh} &= (2^{\Delta GR \cdot G_{cur}} - 1) / (2^{G_{cur}} - 1) \\
 \Delta GR &= (GR - GR_{min}) / (GR_{max} - GR_{min})
 \end{aligned} \right\} (49)$$

where ε and δ are rock anisotropy parameters of the formation at any measured depth; ε_c and δ_c are rock anisotropy parameters of the shale section; V_{sh} is the shale content, %; GR is gamma ray value; GR_{max} is the maximum value of gamma ray; GR_{min} is the minimum value of gamma ray; G_{cur} is the Hilchie index whose value is 3.7 for the Neogene Stratigraphy and 2 for old strata.

After obtaining the rock anisotropy parameters (ε and δ), we can calculate the acoustic wave perpendicular to the bedding plane of the formation by using the inversion method

shown in Fig.7 and the well logging data of acoustic wave. Thus, the rock drillability anisotropy of the formation can be calculated by equations (46) & (47), and the corresponding anisotropic drilling characteristics can be evaluated by equations (8) & (9), as shown in figure 9.

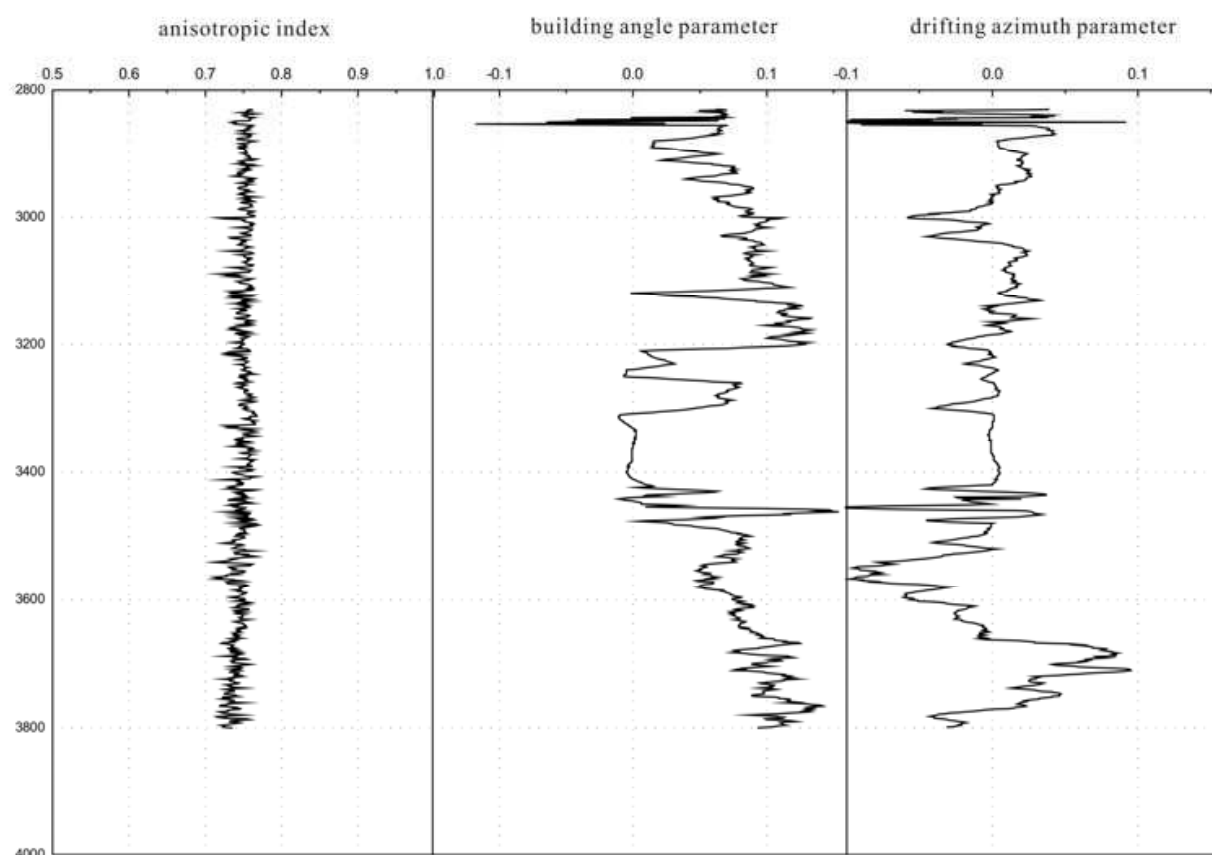


Fig. 9. The evaluation results of anisotropic drilling characteristics of the formation at the Honggouzi conformation in Qinghai oilfield

6. Conclusion

The orthotropic formation and the transversely isotropic formation are the typical formations encountered frequently in drilling engineering. Based on rock-bit interaction model, the two parameter equations have been derived for us to calculate the anisotropic drilling characteristics of them as soon as rock drillability anisotropy of the formations is evaluated quantitatively by using the oilfield data.

The correlation between rock drillability anisotropy and acoustic wave anisotropy of the formation can be matched to each other by an exponential function which is of the best extrapolative performance and relativity. Coefficients in the model are various for different formations to be drilled.

To a certain extent, the research results presented here have shown a new way for us to evaluate conveniently rock drillability anisotropy of the formation by using well logging or seismic data. Case study shows that this evaluation method is better for applications of rock drillability anisotropy of the formation in drilling engineering.

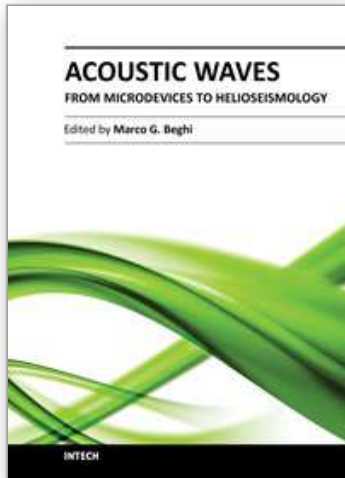
7. Acknowledgment

The authors are grateful for the financial support from the national research project (Grant No. 2010CB226703) and the supply of many core samples by CCSD.

8. References

- Gao, D.; Dai, D. & Pan, Q. (2008). Evaluation of deflecting characteristics of anisotropy formation by using well-log information. *ACTA PETROLEI SINICA*, Vol.29, No.6, (December 2008), pp. 927-932, ISSN 0253-2697
- Gao, D. & Pan, Q.(2006). Experimental study of rock drill-ability anisotropy by acoustic velocity. *Petroleum Science*, Vol. 3, No.1, (March 2006), pp.50-55, ISSN 1672-5107
- Gao, D. (1995). Predicting and scanning of wellbore trajectory in horizontal well using advanced model. *Proceedings of the Fifth International Conference on Petroleum Engineering Held in Beijing, China*, SPE 29982, pp.297-308, 14-17 Nov. 1995
- Gao, D.; Liu, X. & Xu B.(Dec. 1994). *Prediction and Control of Well Trajectory*, Petroleum University Press, ISBN 7-5636-0584-3/TE-95, Dongying, China
- Gao, D. & Liu, X.(1990). Anisotropic drilling characteristics of the typical formations. *Journal of the University of petroleum, China*, Vol.14, No.5, (Oct. 1990), pp.1-8, ISSN 1000-7393
- Gao, D. & Liu, X.(1989). A new model of rock-bit interaction. *Oil Drilling and Production Technology*, Vol.11, No.5, (Oct. 1989), pp.23-28, ISSN 1000-7393
- Lubinski, A. & Woods,H.(1953). Factors affecting the angle of inclination and dog-legging in rotary bore holes. *DPP*, 1953: 222-242
- Patrick, J. & Richard L.(1984). An experimental test of P-wave anisotropy in stratified media. *Geophysics*, Vol.49,No.4, (1984),pp. 374-378
- Xu, B.(Jan. 2011). *Concise Elasticity and Plasticity*, Higher Education Press, ISBN 978-7-04-030725-2, Beijing, China
- Yin H.(1989). Study of formation anisotropy-rock drillability. *Oil Drilling and Production Technology*, Vol.11, No.1, (Feb. 1989),pp.15-22, ISSN 1000-7393

IntechOpen



Acoustic Waves - From Microdevices to Helioseismology

Edited by Prof. Marco G. Beghi

ISBN 978-953-307-572-3

Hard cover, 652 pages

Publisher InTech

Published online 14, November, 2011

Published in print edition November, 2011

The concept of acoustic wave is a pervasive one, which emerges in any type of medium, from solids to plasmas, at length and time scales ranging from sub-micrometric layers in microdevices to seismic waves in the Sun's interior. This book presents several aspects of the active research ongoing in this field. Theoretical efforts are leading to a deeper understanding of phenomena, also in complicated environments like the solar surface boundary. Acoustic waves are a flexible probe to investigate the properties of very different systems, from thin inorganic layers to ripening cheese to biological systems. Acoustic waves are also a tool to manipulate matter, from the delicate evaporation of biomolecules to be analysed, to the phase transitions induced by intense shock waves. And a whole class of widespread microdevices, including filters and sensors, is based on the behaviour of acoustic waves propagating in thin layers. The search for better performances is driving to new materials for these devices, and to more refined tools for their analysis.

How to reference

In order to correctly reference this scholarly work, feel free to copy and paste the following:

Deli Gao and Qifeng Pan (2011). Evaluation Method for Anisotropic Drilling Characteristics of the Formation by Using Acoustic Wave Information, *Acoustic Waves - From Microdevices to Helioseismology*, Prof. Marco G. Beghi (Ed.), ISBN: 978-953-307-572-3, InTech, Available from: <http://www.intechopen.com/books/acoustic-waves-from-microdevices-to-helioseismology/evaluation-method-for-anisotropic-drilling-characteristics-of-the-formation-by-using-acoustic-wave-i>

INTECH
open science | open minds

InTech Europe

University Campus STeP Ri
Slavka Krautzeka 83/A
51000 Rijeka, Croatia
Phone: +385 (51) 770 447
Fax: +385 (51) 686 166
www.intechopen.com

InTech China

Unit 405, Office Block, Hotel Equatorial Shanghai
No.65, Yan An Road (West), Shanghai, 200040, China
中国上海市延安西路65号上海国际贵都大饭店办公楼405单元
Phone: +86-21-62489820
Fax: +86-21-62489821

© 2011 The Author(s). Licensee IntechOpen. This is an open access article distributed under the terms of the [Creative Commons Attribution 3.0 License](#), which permits unrestricted use, distribution, and reproduction in any medium, provided the original work is properly cited.

IntechOpen

IntechOpen